Micromechanical Characteristics of Flux-Grown SmAlO$_3$ Single Crystal

K. K. Bamzai,[a] Vishal Singh,[a] Nidhi,[a] P. N. Kotru,[a] and B. M. Wanklyn[b]

[a] Crystal Growth and Material Research Laboratory, University of Jammu, India

[b] Clarendon Laboratory, Oxford University, UK

Микромеханические характеристики монокристалла SmAlO$_3$, выращенного из расплава

К. К Бамзай[a], Вишал Сингх[a], Нидхи[a], П. Н. Котру[a], Б. М. Ванклин[б]

[a] Лаборатория кристаллографии и материаловедения, Университет г. Джамму, Индия

[б] Кларендонская лаборатория, Оксфордский университет, Великобритания

Представлены результаты определения механических характеристик монокристаллов алюмината самария (SmAlO$_3$) путем индентирования в диапазоне сжимающих нагрузок 0,098... ...0,98 Н. Установлена нелинейная зависимость микротвердости от уровня нагрузки, которая соответствует закону Хейза–Кенделла. Использование этого закона позволяет рассчитать значение твердости, инвариантное к уровню нагрузки. При индентировании микрокристаллов трещинообразование наблюдается только при высоких нагрузках (> 0.686 Н), причем конфигурация инициируемых трещин относится к типу Палмквиста. Для монокристаллов SmAlO$_3$ по результатам измерения твердости и растрескивания при индентировании оценены вязкость разрушения K_c, показатель хрупкости B_i и предел текучести $\sigma_\text{т}$.

Ключевые слова: микропрочность, трещина, разрушение, монокристалл алюмината самария SmAlO$_3$.

Introduction. Aluminates are interesting series within which at room temperature there exist compounds belonging to at least two different structure types. Rare earth based oxides occupy an important place among the materials having high temperature application [1]. Rare earth aluminates serve as neutron absorber, flux suppressers and high temperature container materials. These materials are also of considerable interest on account of their magnetic and optical properties [2]. Thermal conductivity of the aluminates of samarium and dysprosium was investigated employing laser flash technique covering a temperature range from 673 to 1373 K [3]. Raman spectra of an oriented single crystal of SmAlO$_3$ have been obtained at temperature 10–970 K [4]. Etching kinetics and assessment of defect was carried out by Bamzai et al. [5] at different temperatures viz., 443 to 523 K on ErAlO$_3$ crystal where as fracture mechanics, crack propagation and hardness on ErAlO$_3$ as well as DyAlO$_3$ crystals were also reported by the same author [6, 7].

Microhardness is one of the important mechanical property of materials and its measurement include diverse properties like Young's modulus, bulk modulus, dislocation contents and their configuration etc. It is now well-accepted fact that hardness is a measure of the resistance that a lattice offers to the motion of dislocations and deformation. As the hardness properties are related to the crystal structure of the material [8], so microhardness studies have been applied to understand the strength and deformation characteristics of the material. The interest in the microhardness studies does not only result from a technical point of view but also from the opportunity to characterize the degree of lattice order of single crystalline material by microhardness. Indentation-induced microhardness testing studies provide useful information about the mechanical behavior of different materials. It is also strongly related to structure and composition of solids. It is well-known that the microhardness of crystalline material is influenced by the following factors [9]:

1. Solid solution effects connected with the chemical nature of the implanted atoms.

2. Defects aggregates and amorphous region.

3. Point defects, which hinder the motion of dislocations.

The above factors suggest that hardness is a strength microprobe. Kotru et al. [10] carried out microhardness measurement on the crystals of flux-grown rare earth perovskite (RFeO$_3$, R = Gd, Ho, Tb, Dy, Er, and Yb; RCrO$_3$, R = La, Eu, and Dy; RAlO$_3$, R = La, Eu, Gd, and Ho). They re-affirmed the application of the idea of material resistance pressure in the law proposed by Hays and Kendall [11] in the explanation of hardness results. To the best of our knowledge, no results regarding microhardness, crack propagation, fracture toughness and brittleness index of SmAlO$_3$ crystals have been reported. The aim of the present investigation is to report the detailed analysis of microhardness and the laws governing the variation of hardness with applied load. In addition, the present study also discusses the indentation-induced crack propagation; thereby giving values of the fracture toughness, brittleness index and yield strength.

1. **Experimental**.

1.1. *Sample Preparation*. The single crystals of SmAlO$_3$ have been grown by flux technique [12] using PbO, PbF$_2$ as flux, heated in a crucible upto 1290℃, soaked for 24 h and then allowed to cool. Flux grown SmAlO$_3$ single crystal belongs to distorted orthorhombic with lattice parameter $a = 5.285$Å, $b = 5.290$Å, and $c = 7.473$Å with 208.9Å^3 as volume per unit cell [13]. Flux-grown SmAlO$_3$ single crystals, microscopically free from sign of any damage, were selected and properly cleaned with CCl$_4$ and then mounted on galva for indentation purposes.

1.2. *Indentation Tests*. The indentations were performed at room temperature (25℃) using Vickers' microhardness tester (mhp-100) equipped with diamond indenter attached to an incident light camera microscope (Neophot-2 of Carl Zeiss, Germany). On having confirmed that hardness is independent of time, loads ranging from 0.098 to 0.98 N were used for indentation, keeping the indenter at right angle to the surface for 10 s in all cases. At least five indentations were performed for each load on each sample. The distances between two consecutive indentations were kept more than five times the diagonal length of indentation mark to avoid the surface effects. Precautions were taken to ensure that the axis of

the indenter was at right angle to the plane of crystals. Diagonal lengths of these marks were measured using filar micrometer eyepiece at a magnification of $\times 500$ and averages of the diagonal lengths were computed for calculations. The micro-hardness value (H_V) was calculated using formula

$$H_V = 2\sin 68°(P/d^2) \qquad (1)$$

or

$$H_V = 1.8544(P/d^2), \qquad (2)$$

where P is the applied load (in N) and d is the average diagonal length of indentation mark (in μm). The error on H_V was estimated through the relation

$$\Delta H_V = 1.8544[(\Delta P/Y)^2 + (P\Delta Y/Y^2)]^{1/2}, \qquad (3)$$

where $Y = d^2$, $\Delta Y = 2d\Delta d$, ΔP, ΔY, and Δd denote errors on P, Y, and d, respectively.

For each measurement only well-defined cracks developed during indentations were considered and the average crack lengths of all such cracks were taken for a particular indentation impression. The crack length was measured from the centre of the indentation mark to the tip of crack. A program in Fortran 77 using the least square method was written and run on computer to calculate the values of various parameters listed in Table 1.

T a b l e 1

Results of Microhardness Analysis for SmAlO$_3$

H_V, GN·m^{-2}	n_K	n_{HK}	K_1, GN·m^{-2}	W/K_1, 10^{-12} m^{-2}	K_2/K_1	K_2, GN·m^{-2}	W, N
12.45–16.69	1.75	1.92	12.62	3.24	0.52	6.59	0.0409

Comment: n_K represents the value of n on operation of Kick's law ($P = K_1 d^n$) and n_{HK} represents the value of n on operation of the Hays–Kendall law ($P - W = K_2 d^2$).

The fracture toughness (K_c), the brittleness index (B_i), and the yield strength (σ_Y) were determined using the relevant expressions.

2. **Results and Discussion**.

2.1. *Effect of Indentation Time on Vickers' Microhardness*. Hardness of some crystals are reported to be independent of time [14], where as in some others it is shown to be dependent on time [15–17]. In the present case, the impression obtained with a constant load of 10 s, 30 s, 60 s, 2 min, 4 min, 8 min, and 10 min on the selected faces lead to the conclusion that the microhardness in this case is independent of loading time at room temperature.

2.2. *Load Dependence of Hardness*. Various materials behave differently so far as the dependence of their microhardness on applied load is concerned. It is reported that microhardness is:

(i) independent of load [18];

(ii) increases or decreases with load [19, 20];

(iii) shows complex variation with change in load [21, 22];

(iv) increases at low loads and decreases at high loads [23].

It is interesting to find how the materials under investigation (SmAlO₃) behave with change in load.

Figure 1 shows the micrographs of the indentation impression taken at various loads (i.e., lower as well as higher). It is clear from Fig. 1 that size of the indentation mark increases with the increase in applied load. Figure 2 is a graph showing variation of microhardness value with applied load. This value of microhardness H_V is found to vary from 16.69 to 12.45 $\mathrm{GN \cdot m^{-2}}$ at the load ranging from 0.098–0.98 N. The curve in the graph shows that microhardness value decreases nonlinearly as the applied load increases until about 0.686 N of applied load after which microhardness value tends to attain saturation. This particular behavior can be qualitatively explained on the basis of the indenter penetration depth. At small load, the indenter penetrates layers which are nearer to the exposed surface under indentation, and small volumes are stressed. However, as the depth of the penetration increases, the effect of inner layers become more and more prominent and larger volume are stressed resulting into a more or less constant value of hardness with load [24]. This explanation is also favored by Brookes [16], who associated the hardness increase at low loads with early stages of plastic deformation.
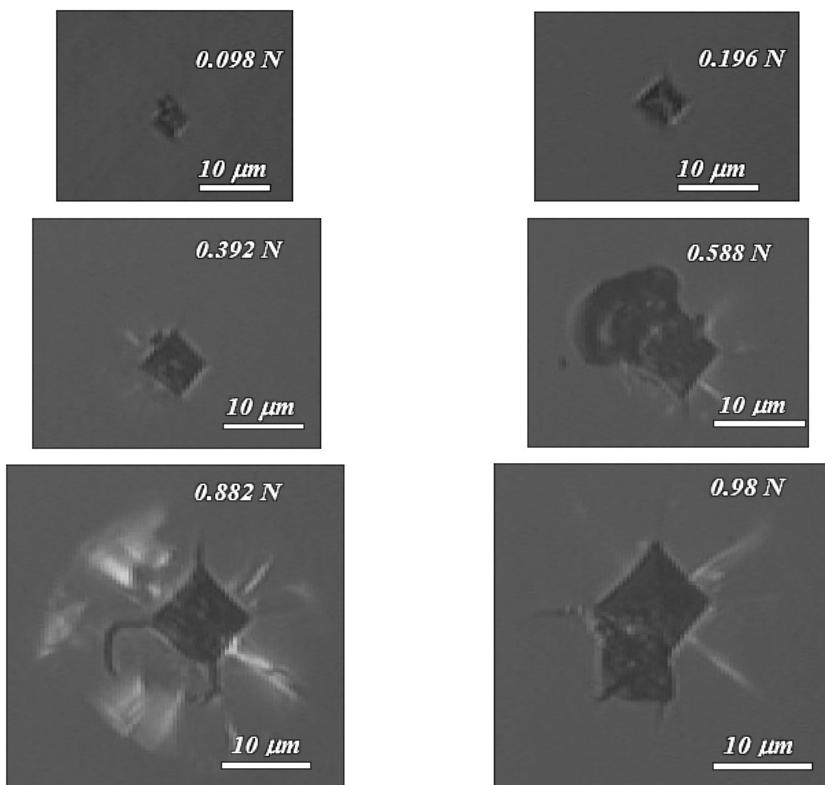

Fig. 1. Micrographs showing indentation impressions at different loads.
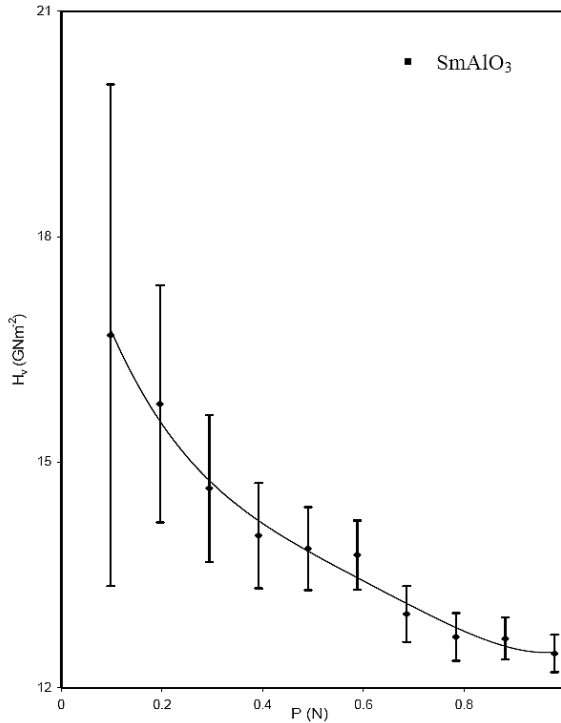
Fig. 2. Graph between microhardness (H_V) and load (P) showing the nonlinear behavior of the SmAlO$_3$ single crystal.

2.3. *Application of the Hays–Kendall Law.* This type of nonlinear behavior is explained by the Hays–Kendall law [11], which is a modification of Kick's law [25],

$$P = K_1 d^n, \tag{4}$$

where K_1 is the standard hardness constant and n is Mayer's index (or work-hardening coefficient), which is assumed to be equal to 2. However, in case of SmAlO$_3$ crystal, the value of n was found to be less than 2 (i.e., $n = 1.75$). This discrepancy was explained by using the Hays–Kendall law which implies that

$$P - W = K_2 d^2, \tag{5}$$

where W is the sample resistance pressure and represents the minimum load that causes an indentation, K_2 is a constant, and $n = 2$ is the logarithmic index.

From (5) we have

$$W = P - K_2 d^2. \tag{6}$$

Substituting the value of (4) in (6), we have

$$W = K_1 d^n - K_2 d^2$$

or

$$d^n = (K_2/K_1)d^2 + W/K_1. \tag{7}$$

A graph of $\log P$ versus $\log d$ is shown in Fig. 3. From this graph slope n and intercept K_1 is calculated. The values of K_2 and W can be calculated from a graph between d^n and d^2 as shown in Fig. 4. The values of these constants have been determined by using the least square fitting method using a software program in Fortran language. A plot of $\log(P - W)$ vs. $\log d$ as shown in Fig. 5 yields the value of $n = 2$ thereby involving concept of resistance pressure (W) as proposed by Hays and Kendall. The data on n_K (on application of Kick's law), n_{HK} (on application of the Hays–Kendall law), K_1, K_2, and W thus determined is given in the Table 1.
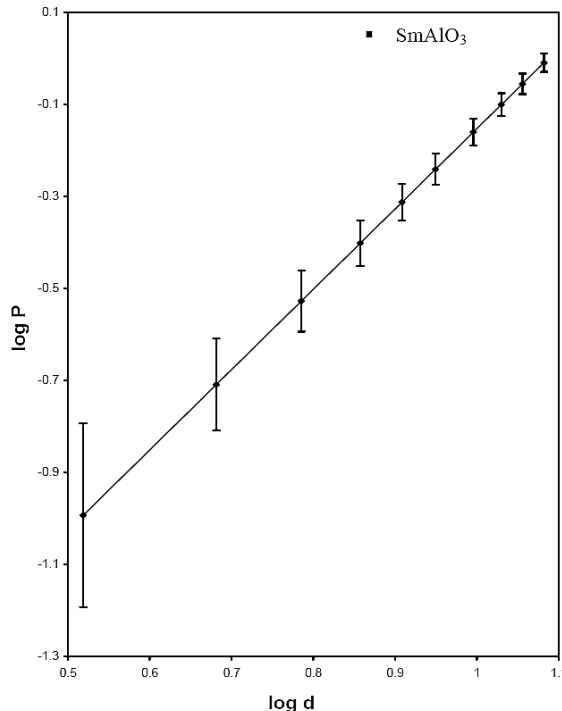

Fig. 3. A linear graph $\log P$ vs. $\log d$ giving the value of slope n and intercept K_1.

The application of the Hays–Kendall law leads us to a modified formula of Eq. (1), which gives load-independent value of microhardness $(H_V)_{l.i}$:

$$(H_V)_{l.i} = 1.8544(P - W)/d^2 \tag{8}$$

or

$$(H_V)_{l.i} = 1.8544K_2. \tag{9}$$

Knowing the value of K_2, the load independent values are calculated using the above relation which comes out to be 12.23 GN·m^{-2}. This load-independent value is in quite good agreement with the experimental values where the saturation in the values of hardness is obtained at higher loads.
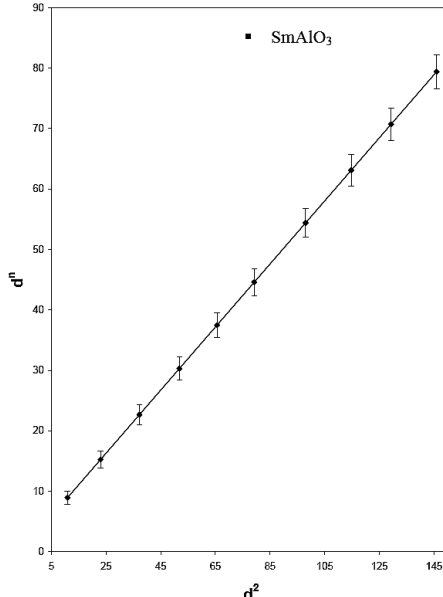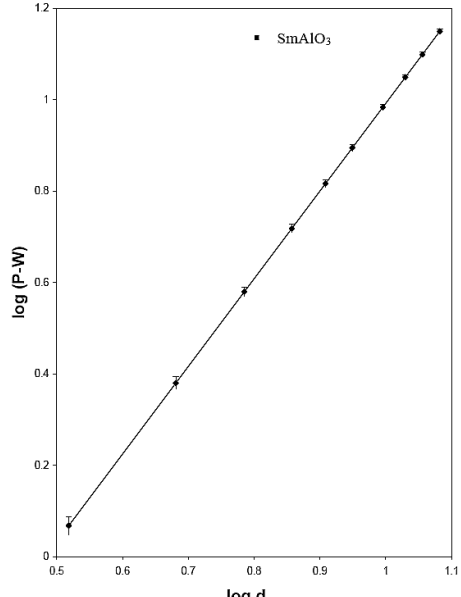
Fig. 4

Fig. 5

Fig. 4. Graph d^n vs. d^2 giving the value of slope K_2 and intercept W/K_1.

Fig. 5. Graph $\log(P - W)$ vs. $\log d$ giving the value of slope $n = 2$.

2.4. *Fracture Mechanics*. There are two modeling approaches to the crack systems, which can develop in material as a result of indentation. These are: (i) median or half penny cracks and (ii) Palmqvist cracks system shown schematically in Fig. 6, respectively.

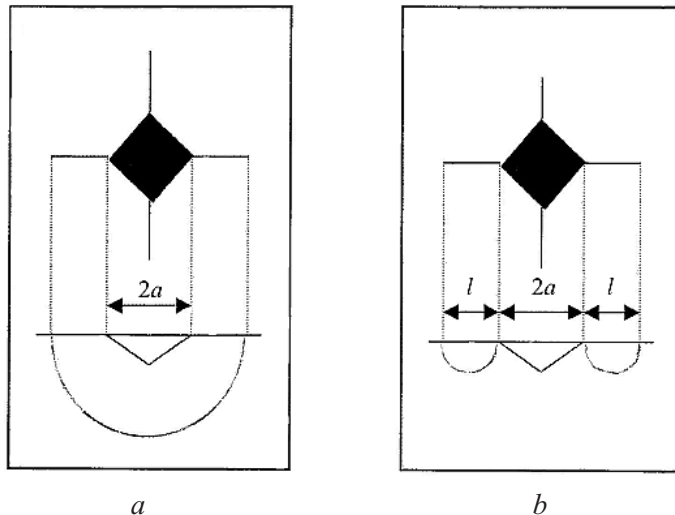*a*   *b*

Fig. 6. Geometries of median (*a*) and Palmqvist crack (*b*) around Vickers indentation.

Thus, depending upon which of those two modules they are based on, various indentation toughness equations in the literature are referred to as half penny or

Palmqvist equations. Resistance to fracture indicates the toughness of material. The fracture toughness (K_c) determines the fracture stress level applied under uniform loading and is important property for selection of materials for application where the load exceeds the limit or yield point.

In the flux-grown SmAlO₃ crystal, no cracks are detected at loads less than 0.588 N. The indentation load for crack initiation reflects the intrinsic deformation and fracture properties of the material [26–28]. The crack developed in a crystal determines the fracture toughness K_c. If P is the applied load (in N) and c is the crack length (in μm), then under equilibrium conditions [29]:

$$K_c = P\big/\beta_0 c^{3/2} \qquad \text{for} \quad c \geq d/2. \qquad (10)$$

Here β_0 is numerical constant that depends upon the indenter geometry. For Vickers' indenter β_0 is equal to 7. However, this equation gives a satisfactory value of the fracture toughness only if $c/a \geq 2.5$ (where $a = d/2$), that is for median cracks [30, 31]. The crack system with $c/a < 2.5$ is a Palmqvist or radial crack. The fracture toughness for a Palmqvist crack system may be calculated by

$$K_c = P\big/\beta_0 a l^{1/2}, \qquad (11)$$

where l is the mean Palmqvist crack length [32], $l = c - a$.

Table 2 gives the c/a value for SmAlO₃ crystal. As the ratio of c/a in the present case is found to be less than 2.5, the cracks developed are Palmqvist in nature. Accordingly Eq. (11) is used to calculate the value of fracture toughness K_c. The value K_c in case of SmAlO₃ crystal has been found to vary between 5.06 to $2.31 \cdot 10^{-2}$ GN $\cdot$ m$^{-3/2}$ for the loads ranging from 0.686 to 0.98 N and is given in Table 2.

T a b l e 2
Vickers' Hardness Value (H_V), Nature of Cracks, Fracture Toughness (K_c),
Brittleness Index (B_i), and Yield Strength (σ_Y)

P, N	H_V, GN $\cdot$ m^{-2}	c/a	Nature of crack	K_c, 10^{-2} GN $\cdot$ m$^{-3/2}$	B_i, m$^{-1/2}$	σ_Y, GN $\cdot$ m^{-2}
0.098	16.69	–	–	–	–	5.56
0.196	15.78	–	–	–	–	5.26
0.294	14.65	–	–	–	–	4.88
0.392	14.02	–	–	–	–	4.67
0.490	13.85	–	–	–	–	4.62
0.588	13.77	–	–	–	–	4.54
0.686	12.98	1.06	Palmqvist	5.06	2565	4.33
0.784	12.67	1.12	Palmqvist	3.64	3476	4.22
0.882	12.65	1.26	Palmqvist	2.52	5019	4.22
0.980	12.45	1.32	Palmqvist	2.31	5373	4.15

A graph of crack length c versus load P is shown in Fig. 7, which indicates the dependence of crack length on applied load. It is clear that the crack length increases with the increase in applied load.
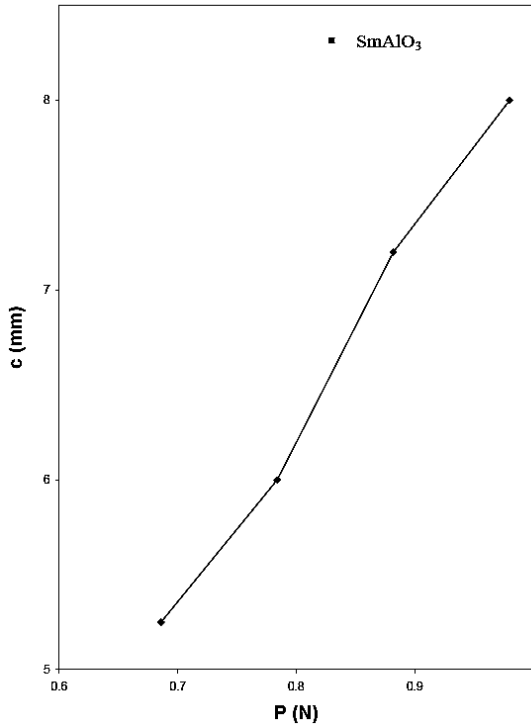

Fig. 7. Graph between crack length and load shows increase in crack length with increase in applied load.

2.5. *Brittleness Index*. Another important mechanical parameter is the brittleness index that affects the mechanical behavior of a material and gives an idea about the fracture induced in a material without any appreciable deformation. The value of brittleness index (B_i) is calculated by using relation [31]

$$B_i = H_V / K_c. \tag{12}$$

The value of B_i is found to vary between 2565 to 5373 m$^{-1/2}$ for the load ranging from 0.686 to 0.98 N, respectively, and is given in Table 2.

2.6. *Yield Strength*. From the hardness value, the yield strength (σ_Y) can be calculated [33].

For Mayer's index $n > 2$, the yield strength is given by

$$\sigma_Y = H_V / 2.9 [1 - (n-2)] \{12.5(n-2)/1 - (n-2)\}^{n-2}. \tag{13}$$

For Mayer's index $n < 2$ [34], the yield strength becomes:

$$\sigma_Y = H_V / 3. \tag{14}$$

Since, in the present case, n is less than 2 (i.e., $n = 1.92$), the Eq. (14) is applied to calculate the value of yield strength and the above values vary from 5.56 to 4.15 GN$\cdot$m^{-2} in the load range from 0.098 to 0.98 N and are given in Table 2.

Table 2 contains compiled data including Vickers' hardness value, nature of crack, fracture toughness, brittleness index and yield strength in case of SmAlO₃ crystal.

C o n c l u s i o n s

1. The variation of microhardness with applied load is non linear and fits into the concept of Newtonian resistance pressure as proposed by the Hays–Kendall law. The Vickers' hardness value of SmAlO₃ crystals in the load range of 0.098 to 0.98 N is of the order of 16.69 to 12.45 GN$\cdot$m^{-2}.

2. Application of the Hays–Kendall law suggests that the load-independent value of microhardness H_V for SmAlO₃ crystals is 12.23 GN$\cdot$m^{-2}. The calculated load-independent values of microhardness fit very well with the experimental ones.

3. The crack is initiated at an applied load of 0.686 N and the nature of cracks is of Palmqvist type for loads ranging from 0.686 to 0.98 N.

4. The fracture toughness value varies from $5.06\cdot10^{-2}$ to $2.31\cdot10^{-2}$ GN$\cdot$m$^{-3/2}$ for the load ranging from 0.686 to 0.98 N, respectively, whereas the brittleness index in this load range varies from 2565 to 5373 m$^{-1/2}$, respectively.

5. The value of yield strength as calculated from $H_V/3$ comes out to be 5.56 to 4.15 GN$\cdot$m^{-2} in the load range of 0.898 to 0.98 N, respectively.

Р е з ю м е

Представлено результати визначення механічних характеристик монокристалів алюмінату самарію (SmAlO₃) шляхом індентування в інтервалі навантаження стиском 0,098...0,98 Н. Установлено нелінійну залежність мікротвердості від рівня навантаження, яке відповідає закону Хейза–Кенделла. За допомогою цього закону можна розрахувати значення твердості, інваріантне до рівня навантаження. При індентуванні мікрокристалів тріщиноутворення має місце за високого навантаження (>0,686 Н), причому конфігурація ініційованих тріщин відноситься до типу Палмквіста. Для монокристалів SmAlO₃ за результатами вимірювання твердості і розтріскування при індентуванні оцінено в'язкість руйнування K_c, показник крихкості B_i і границю текучості $\sigma_{\text{ò}}$.

1. J. D. Cashion, A. H. Cooke, J. M. Leask, et al. "Crystal growth and magnetic susceptibility of some rare earth compounds," *J. Mat. Sci.*, **3**, 402–407 (1968).

2. W. K. Anderson, "Nuclear applications of yttrium and lanthanon," in: F. H. Speeddingand and A. Hdaane (Eds.), Krieger Publishing Co., Huntington, New York (1971), p. 522.

3. G. Suresh, G. Seenivasan, M. V. Krishanaiah, and P. S. Murti, "Investgation of thermal conductivity of selected rare earth aluminates," *J. Therm. Anal.*, **54**, 873–879 (1998).

4. J. F. Scott and J. P. Rameika, "High temperature Raman study of samarium aluminate," *Phys. Rev. B*, **1**, 4182–4185 (1970).

5. K. K. Bamzai, P. R. Dhar, P. N. Kotru, and B. M. Wanklyn, "Studies on etching kinetics and assessment of defects in flux grown $ErAlO_3$," *Mat. Chem. Phys.*, **62**, 214–225 (2000).

6. K. K. Bamzai, P. N. Kotru, and B. M. Wanklyn, "Fracture mechanics, crack propogation and microhardness studies on $ErAlO_3$ single crystal," *J. Mat. Sci. Technol.*, **16**, 405–410 (2000).

7. K. K. Bamzai, P. R. Dhar, P. N. Kotru, and B. M. Wanklyn, "Investigations on indentation induced hardness and fractured mechanism in flux grown $DyAlO_3$ crystal," *Appl. Surf. Sci.*, **133**, 195–204 (1998).

8. B. W. Mott, *Microindentation Hardness Testing*, Butterworths Scientific Publication, London (1956).

9. T. Hioki, A. Itoh, M. Ohkubo, et al. "Mechanical property changes in sapphire by nickel ion implantation and their dependence on implantation temperature," *J. Mat. Sci.*, **21**, 1321–1328 (1986).

10. P. N. Kotru, K. K. Raina, and S. K. Kachroo, "Microhardness measurements on single crystals of flux-grown rare earth perovskites (orthoferrites, orthochromites and aluminates)," *Ibid*, **19**, 2582–2592 (1984).

11. C. Hays and E. G. Kendall, "An analysis of Knoop microhardness," *Metallography*, **6**, 275–282 (1973).

12. B. M. Wanklyn, "The flux growth of single crystal of rare earth perovskite (orthoferrites, orthochromites and aluminates)," *J. Cryst. Growth*, **5**, 323–328 (1969).

13. S. Geller and V. B. Bala, "Crystallographic studies of perovskite like compounds. II. Rare earth aluminate," *Acta. Cryst.*, **9**, 1019–1025 (1956).

14. S. Beigh, P. N. Kotru, and B. M. Wanklyn, "Indentation induced microhardness studies on (110) and (001) phase of flux grown dysprosium orthoferrite single crystal," *Mat. Chem. Phys.*, **40**, 99–104 (1995).

15. V. P. Bhatt and C. F. Desai, "Temperature dependence of Vicker microhardness and creep of InBi single crystal," *Bull. Mater. Sci.*, **4**, 23–28 (1982).

16. C. A. Brookes, "The mechanical properties of cubic boron nitride – a perspective view," 2nd Int. Conf. on *Hard Materials* (Rhodes, Greece, Sept. 23–28, 1984), Inst. Phys. Conf. Ser. 75, Ch. 3, Hilger, Bristol (1984), pp. 207–220.

17. Y. Deslandes, E. Alva Rosa, F. Brisse, and T. Meneghini, "Correlation of microhardness and morphology of poly (ether-ether-ketone) films," *J. Mat. Sci.*, **26**, 2769–2777 (1991).

18. C. Ascheron, G. Kuhn, C. Haase, and H. Neumann, "Microhardness of Sn-doped InP, *Cryst. Res. Technol.*, **24**, K33–K35 (1989).

19. K. Balakrishan, B. Vengatesan, N. Kanniah, and P. Ramaswami, "Growth and microhardness studies of CuInSe$_2$ single crystal," *J. Mater. Sci. Lett*., **9**, 785–787 (1990).

20. P. N. Kotru, A. K. Razdan, and B. M. Wanklyn, "Microhardness of flux grown pure doped and mixed rare-earth aluminates," *J. Mat. Sci*., **24**, 793–803 (1989).

21. V. P. Bhatt, R. M. Patel, and C. F. Desai, "Deformation and microhardness studies on KClO$_4$ single crystal," *Cryst. Res. Technol*., **18**, 1173–1179 (1983).

22. P. R. Dhar, K. K. Bamzai, and P. N. Kotru, "Deformation and microhardness studies on natural apophyllite crystal," *Ibid*, **32**, 537–544 (1997).

23. D. J. Clinton and R. Morell, "Hardness testing of ceramic material," *Mat. Chem. Phys*., **17**, 461–473 (1987).

24. J. R. Pandya, L. J. Bhagia, and A. J. Shah, "Microhardness of rhombohedral crystal carlcite and sodium nitrate," *Bull. Mater. Sci*., **5**, 79–82 (1983).

25. F. Kick, *Das Gesetz der proportionalen Widerstand und seine Anwendung*, Arthus Felix, Leipzig (1885).

26. H. Ishinkaa and N. Shinkai, "Critical load for median crack initation in Vicker's indentation of glass," *J. Amer. Ceram. Soc*., **65**, C124–C127 (1982).

27. B. R. Lawn and A. G. Evans, "A model for crack initiation in elastic/plastic indentation fields," *J. Mat. Sci*., **12**, 2195–2199 (1977).

28. B. R. Lawn, A. G. Evans, and D. B. Marshall, "Elastic/plastic indentation damage in ceramics: the median/radial crack system," *J. Amer. Ceram. Soc.*, **63**, 574–581 (1980).

29. B. R. Lawn and E. R. Fuller, "Equilibrium penny-like cracks in indentation fracture," *J. Mat. Sci*., **9**, 2016–2024 (1975).

30. D. G. Bhat, "Elastic/plastic indentation damage in ceramics: the median/radial crack system," *J. Amer. Ceram. Soc.*, **64**, 165–166 (1981).

31. K. Nihara, R. Morena, and D. P. H. Hasselman, "Evaluation of K_{Ic} of brittle solids by indentation method with low crack to indent ratios," *J. Mater. Sci. Lett.*, **1**, 13–16 (1982).

32. C. B. Ponton and R. D. Rawling, "Dependence of the Vickers indentation fracture toughness on the surface crack length," *J. Brit. Ceram. Trans*., **88**, 83–90 (1989).

33. J. P. Cahoon, W. H. Broughton, and A. R. Katzuk, "The determination of yield strength from hardness measurement," *Metall. Trans*., **2**, 979–983 (1971).

34. D. H. Wytt, *Metals, Ceramics, and Polymers*, Cambridge University Press, London, (1974).